

Lognormally Distributed K/Th/U Concentrations – Evidence for GeoCritical Fracture Flow, Los Azufres Geothermal Field, MX

Peter Leary¹, Peter Malin¹, Eylon Shalev¹, Graham A. Ryan¹,
Cecilia Lorenzo², and Magaly Flores²

¹Institute of Earth Science & Engineering, University of Auckland, NZ

²Comisión Federal de Electricidad, Morelia, MX

cecilia.lorenzo@cfe.gob.mx • p.leary@auckland.ac.nz

Keywords

Fractures, percolation flow, fracture-connectivity, well-logs, lognormality

ABSTRACT

Well-log data for solute species K, Th and U for two wells in the Los Azufres geothermal field in central Mexico show lognormal population distribution systematics that can be understood in terms of *in situ* fracture-borne flow in a ‘geocritical’ crustal reservoir. Radionuclide solute well-log data could help build large-scale observationally-constrained models of *in situ* flow structures within a geocritical reservoir.

Well-log, well-core, and field permeability data for crustal rock can be unified into an empirical/physical scheme in which *in situ* fracture systems are understood to be long-range spatially-correlated networks of grain-scale fractures/defects through which fluids percolate on all length and time scales. In this ‘geocritical’ model of *in situ* fluid flow, reservoir permeability is controlled by fracture-fracture interactions leading to fracture-connectivity pathways within a background of grain-scale fractures. The greater the fracture connectivity within a crustal volume the greater the permeability and the more lognormally distributed are the fracture-system flow pathway populations. It is thus plausible that significant flow structures in a geothermal reservoir appear as localized solute deposition events within an otherwise normally-distributed solute-abundance population. Lognormal distributions of K/Th/U solute abundances appear at intervals along the Los Azufres spectral gamma well-log fluctuation record, in contrast with more normally-distributed well-log fluctuations elsewhere in the K/Th/U logs and for other logging data (sonic velocity, mass density, neutron porosity). In line with generic geocritical flow phenomenology, K/Th/U lognormality in well-intervals indicates the presence of large-scale *in situ* flow structures which concentrate solute deposition in high-flux channels revealed by the well-log. If such flow structures are currently active, advanced reservoir modeling techniques can incorporate their flow path information into more comprehensive and reliable reservoir-scale flow models.

Introduction

Well-log data recorded in two wells at the Los Azufres geothermal field 60 km east of Morelia, Michoacan, in Mexico’s Central Volcanic Belt (Molina Martinez 2009; Gutierrez & Aumento 1982) are observed to have Fourier power-spectra that scale inversely with spatial frequency k , $S(k) \sim 1/k^\beta$, $\beta \sim 1.4$, over 2.5 decades of scale length, ~ 1 cycle/km $< k < \sim 300$ cycles/km. As such, the Los Azufres well-logs affirm that, in at least some *in situ* physical aspects, geothermal reservoir properties accord with a vast array of well-log data recorded at hydrocarbon reservoirs and scientific deep drill-sites worldwide (Leary 2002). Interpretations of well-log power-law spectral scaling systematics $S(k) \sim 1/k^\beta$, $\beta \sim 1-1.2$, in the crust at large indicate an essentially universal existence of a background population of grain-scale cement-bond fractures within a population of otherwise intact grain-grain cement bonds (Leary 1991, 1997, 2002). (The power-law scaling exponent $\beta \sim 1.4$ at Los Azufres may be biased to higher values than commonly observed, $\beta \sim 1-1.2$, because the geological interfaces are Neogene age versus Mesozoic age and older for most oil /gas field formations; sharp interfaces generate power-law spectra with $\beta = 2$.)

Equally attested in oil/gas field clastic reservoir rock is evidence of well-core poroperm systematics centered on grain-scale fluid percolation flow. Grain-grain cement bond fracture sites conduct crustal fluids by percolation along fracture-connectivity pathways signaled by the relation of *in situ* porosity ϕ to the logarithm of *in situ* permeability κ , $\delta\phi \propto \delta\log(\kappa)$, attested by well-core data from clastic reservoirs (Leary & Al-Kindy 2002; Leary & Walter 2008). Well-core and field-scale populations of permeability data κ can be described as lognormally distributed according to the expression $\kappa(x,y,z) = \kappa_0 \exp(\alpha(\phi(x,y,z) - \phi_0))$, where ϕ is the normally-distributed *in situ* porosity, κ_0 = median permeability, ϕ_0 = median porosity and α = lognormality parameter associated with *in situ* fracture connectivity (Leary et al. 2012ab, 2013).

While no well-core sequences are available for the Los Azufres geothermal field, limited well-core poroperm sequence data from geothermal fields in New Zealand (IESE unpublished data) and the Philippines (Stimac 2007) are consistent with observed oil/gas field poroperm systematics. We thus regard it as plausible

to consider the Los Azufres geothermal field as a member of a large class of *in situ* flow systems having the trio of properties that collectively define a ‘geocritical reservoir’:

- Well-log spectra scale inversely with spatial frequency, $S(k) \sim 1/k^\beta$, $\beta \sim 1$
- Well-core poroperm sequence fluctuation relation $\delta\phi \propto \delta\log(\kappa)$
- Field-scale permeability lognormally distributed as $\kappa(x,y,z) = \kappa_0 \exp(\alpha(\phi(x,y,z) - \phi_0))$.

The spatially-interactive nature of *in situ* fractures in a ‘geocritical reservoir’ leads naturally to lognormal permeability distributions associated with solute abundances as observed within the Los Azufres reservoir; i.e., lognormality is expected for geocritical flow. Well-log spatial evidence for large-scale *in situ* flow structures offers the potential for using observable K, Th and U solute abundances to constrain models of large-scale reservoir flow (Leary et al 2013).

Los Azufres K, Th & U Well-Log Abundances

Two non-producing Los Azufres wells, AZ01D and AZ47D, ~650m apart on either side of a local normal fault (Fig 1, Molina Martinez 2009) were circulated for cooling in order to obtain well log data for the reservoir structure across the fault.

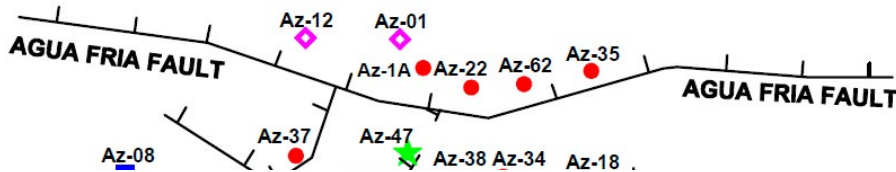


Figure 1. Location sketch for well-sites 01 (magenta diamond) and 47 (green star); wells 01D and 47D are non-producers at these well-sites.

Among the Los Azufres well-logs are spectral gamma, recording the natural gamma ray activity due to nuclear decay of *in situ* potassium isotope K^{40} and members of the thorium Th and uranium U decay chains. Table 1 gives estimated average values for crustal potassium at ~3% abundance, largely in common minerals, with Th and U abundances being ~10ppm and ~3ppm respectively, largely as mobile trace element species resident in upper crustal rock. Some K and most Th and U are associated with crustal fluid movement.

Table 2 profiles aspect of well-log spectral gamma data. Logs spatially resolve gamma emissions for K, Th and U over a 20-30cm window by recording gamma counts/second while traveling at 15cm/s along the wellbore. Gamma count repeatability is ~.25% for K and ~1ppm for Th/U. The resulting data measures *in situ* species abundance to an accuracy of .4% for K, and 3.2ppm and 2.3ppm for Th and U respectively.

Table 1 gamma-active species crustal abundance data show that well-log measurement repeatability of ~1ppm for Th/U is adequate to detect *in situ* species

Table 1. K/Th/U abundances for crustal rock (Clark 1966).

Rock Type	Uranium	Thorium	Potassium
Mafic	0.5 to 1 ppm	3 to 4 ppm	0.80%
Salic	3 ppm	17 ppm	4%
Crustal Average	2.8 ppm	10.7 ppm	2.80%

Table 2. Spectral gamma well-log tool specifications (www.slb.com).

Logging speed 15cm/s
Vertical resolution 20 to 30 cm
K: ±0.4% (accuracy), 0.25% (repeatability)
Th: ±3.2 ppm (accuracy), 1.5 ppm (repeatability)
U: ±2.3 ppm (accuracy), 0.9 ppm (repeatability)

in formations having mean abundances 3ppm for U and 10ppm for Th. Fig 2 shows that whole-log abundances for Th and U in the Los Azufres rock suites are at levels compatible with Table 1 crustal averages: 50ppm for thorium and 5ppm for uranium in well 01D, 5ppm for thorium and 1ppm for uranium in well 47D.

Lognormality Versus Normality in Los Azufres Well-Log Fluctuations

Generally speaking, spatial fluctuations in rock physical properties are normally distributed about a mean value. Fig 2 demonstrates that certain wellbore intervals in Los Azufres field – e.g., the broad spikes at 1.4km depth in well 01D and at 1.35km depth in well 47D -- contain a significant over-abundance of Th and U relative to the background mean occurrence rates. These high-abundance spikes are reflected in high-abundance population tails evident in the abundance distribution histograms. These two diagnostics indicate the existence of a physical process involving Th/U species outside the standard *in situ* processes leading to standard normal population distributions.

Figs 3-4 overlay well-log profiles of Th (blue) and U (red) along with K (black) abundance fluctuations in the Los Azufres crustal sections. To put the different abundance fluctuations on a more equal footing, the well-log traces are normalized to

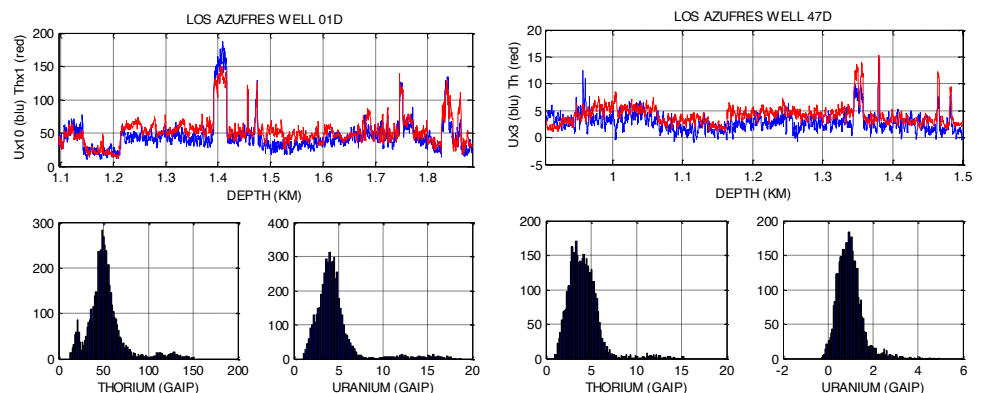


Figure 2. (Upper left/right) Los Azufres geothermal field well-log abundances for Th(blue)/U(red) in wells 01D/47D. (Lower left/right) Whole-well Th/U lognormal well-log abundance distributions for wells 01D/47D. Species abundances given in API units.

zero-mean and unit-variance; trace amplitudes are expressed as standard deviation from the trace means rather than as absolute counts (Figs 2, 6-7 give absolute counts).

The Fig 3-4 Th/U well-log abundance sequences are similar in structure: (i) isolated wellbore intervals have species over-abundance; (ii) normalized over-abundances are equal. The observed over-abundance spikes are annotated by red/blue underscores keyed to well-log intervals showing evidence of lognormal population distributions identified in a well-log interval analysis (illustrated in Fig 12). As a general feature of Fig 3-4, Los Azufres well-log intervals having conspicuous

Th/U abundances are intervals with lognormal Th/U abundance distributions.

The Los Azufres spectral gamma well-log data afford a means of understanding the physical mechanism for creating Th/U solute concentrations leading to the observed *in situ* lognormal distributions of Figs 2-4. While well-log K abundances are less conspicuously associated with lognormal events, a tendency for elevated K in parallel with Th/U events is evident in Figs 3-4. We note that while K is 300-1000 times more abundant than Th or U (~3% versus ~0.003-.01%) relative to the mean, the spatial fluctuations about a zero-mean value are of the same order for each species. It thus makes sense to regard K as having a large static background ‘reservoir’ abundance that accounts for most of the K gamma ray signal, while at the same time there exists a spatially fluctuating mobile solute component comparable in size to and occurring in the same locations as the Th and U species.

Fig 5 makes this point in histogram form. The upper histograms for the two wells (01 to left, 47 to right) show that the K abundances are essentially normally distributed within $\pm 1-1.5$ standard deviations about a zero-mean, as would be expected for a residence mineral distribution. In contrast with the K distributions, and as seen in Fig 2, the Th (center) and U (lower) abundance histograms show significant high-value tails of 5-6 standard deviations from the zero-mean; the bulk of the Th and U lies within ± 1 standard deviations of the mean. The broader 1.5-2 sigma distribution width for K about the mean may reflect mineral processes that don’t affect solute transport. Equally noteworthy in the Well 47D K abundance distribution is the outlier peak 2 standard deviations below the K mean value. This standalone K distribution is likely to be an analog of the Th and U distributions, reflecting a mobile solute K population with its right-hand high-abundance tail buried beneath the populace of the immobile resident K.

The high-value population tails in the Figs 2 & 5 Th/U abundance distributions are in contrast with the greater population of K abundances in Fig 5. Figs 6-7 sustain this contrast between Th/U abundances and the fluctuation population distributions of other *in situ* physical properties recorded in Los Azufres wells. Fig 6 shows that for well 01D, well-log data for electrical resistivity, photoelectric formation factor, mass density and thermal neutron porosity are more or less normally distributed about a central peak at the distribution mean.

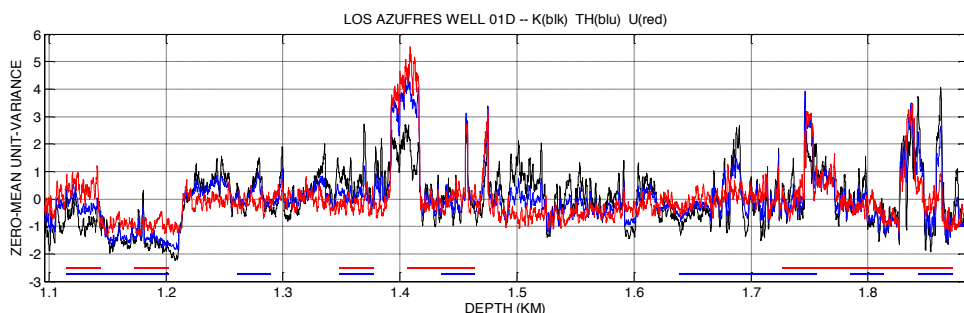


Figure 3. Los Azufres well 01D spectral gamma distribution with well depth; K=black; Th=blue; U=red. Data normalized to zero-mean/unit-variance. Underscores denote well-log intervals in which lognormal distributions of Th/U species abundances are identified.

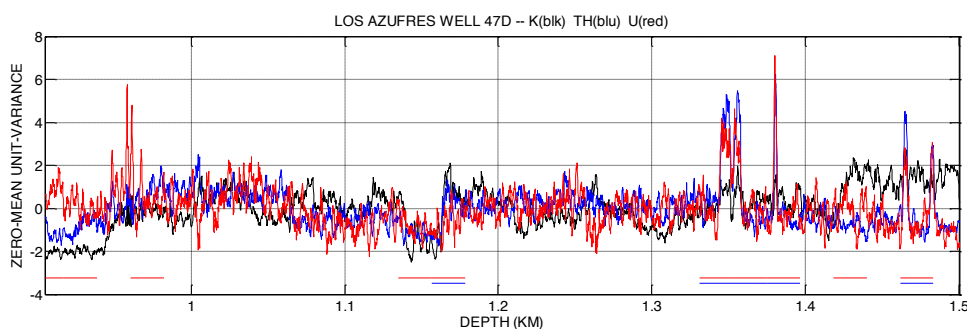


Figure 4. Los Azufres Well 47D spectral gamma distribution with well depth; K=black; Th=blue; U=red. Data normalized to zero-mean/unit-variance. Underscores denote well-log intervals in which lognormal distributions of Th/U species abundances are identified.

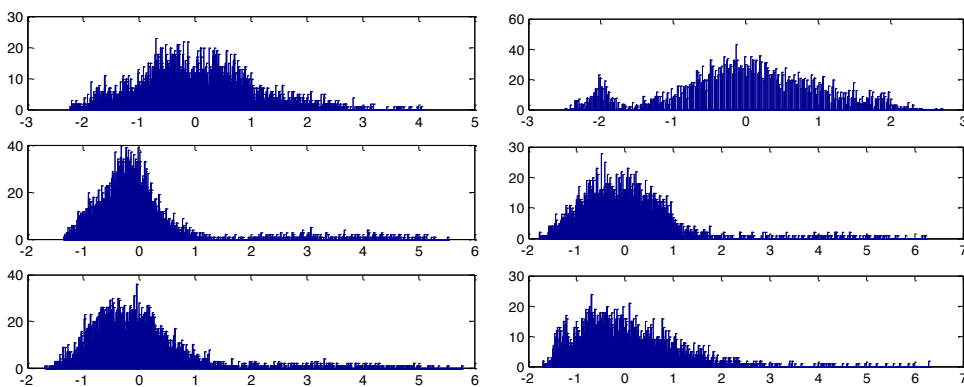


Figure 5. Los Azufres spectral gamma well-log fluctuation histograms; (left/right) Well 01D/47D. Data normalized to zero-mean/unit-variance; K=upper; Th=center; U=lower; high-end lognormal distributions reach 5 to 6 standard deviations for Th/U; well 47D K distribution includes likely analogue to Th/U lognormal distributions as small peak to left of the main normal distribution.

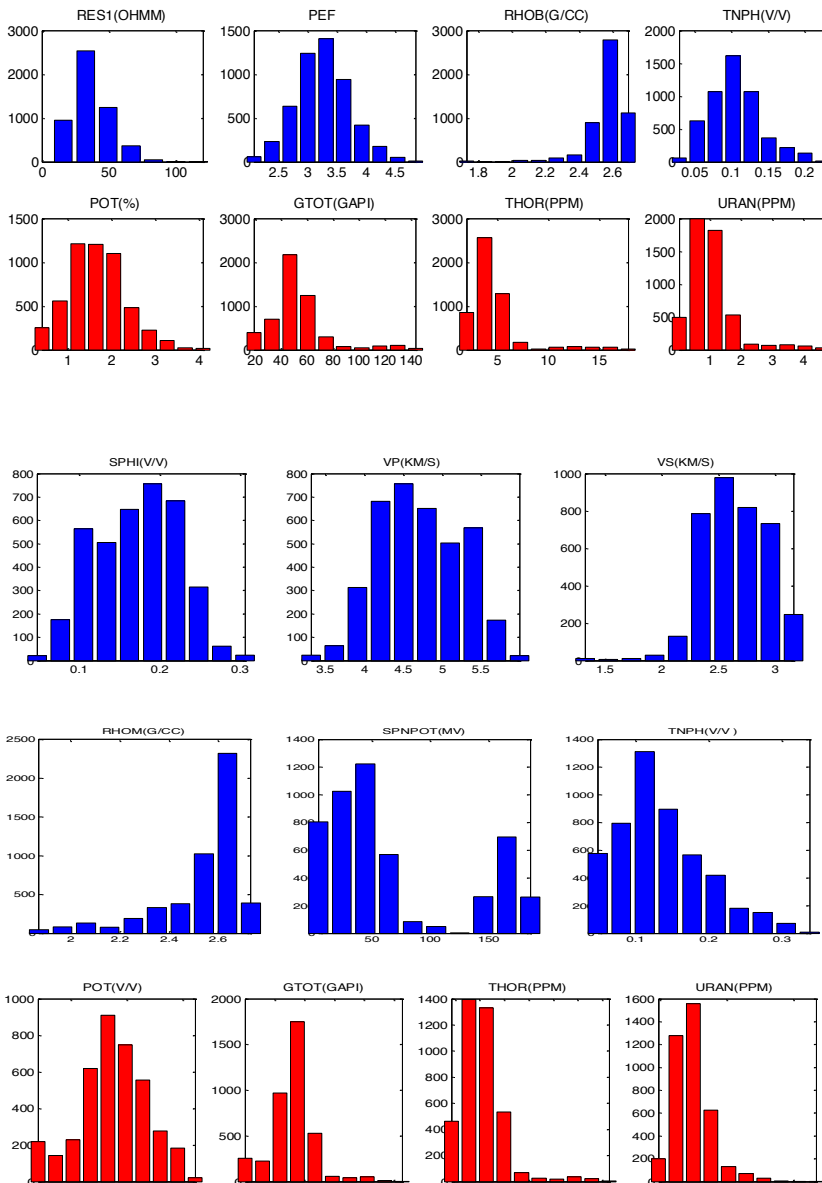


Figure 7. Comparison of Los Azufres well 47D well-log fluctuation histogram tendency for normality for non-gamma variables and lognormality for gamma variables; non-gamma data (blue); gamma data (red).

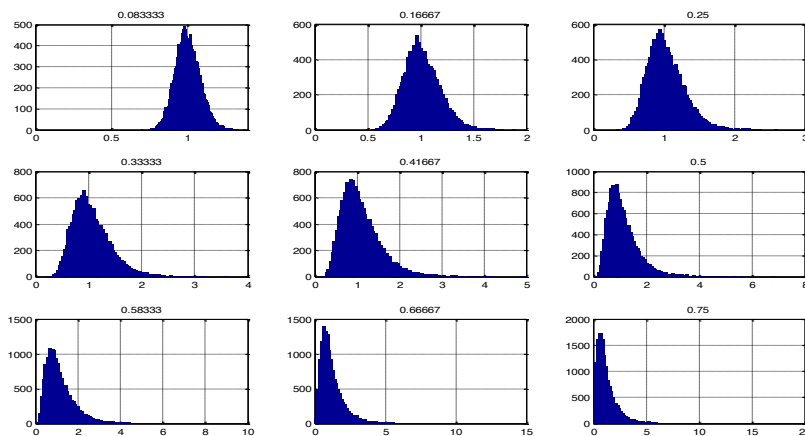


Figure 6. Comparison of Los Azufres well 01D well-log fluctuation histogram tendency for normality for non-gamma variables and lognormality for gamma variables; non-gamma data (blue); gamma data (red).

Similarly, the Fig 7 data for well 47D show sonic porosity (derived from assumed fracture density dependence on velocity), sonic velocity (in part due to variations in fracture density), density, spontaneous potential and thermal neutron porosity similarly have a tendency for normal distributions.

Figs 2-7 loosely associate Th and U, and some instances K, well-log fluctuation populations with lognormal-like high-value tails of 5-6 standard deviations in contrast with the remainder of well-log fluctuations populations having normal population distributions within 1.5-2 standard deviations of the mean. An interval-by-interval analysis of well-log fluctuation distributions (a sample of which appears in Fig 12) tightens the spatial association of lognormal distributions of Th/U populations with well-log intervals having high Th/U deviation from the mean. Well-log intervals are parameterised by (i) $\rho = \text{maximum-abundance/median-abundance}$ and (ii) a lognormality parameter α , an exponential factor controlling the degree of fracture connectivity in the empirical ‘geocriticality’ poroperm relation $\kappa = \kappa_0 \exp(\alpha\phi)$. Fig 8 illustrates the role of parameter α in shaping permeability κ distributions for normally-distributed porosity ϕ ; as α increases, the κ -distributions grow increasingly skewed to left as high permeability values stretch the x-axis to the right.

The empirical poroperm relation $\kappa(x,y,z) = \kappa_0 \exp(\alpha(\phi(x,y,z) - \phi_0))$ is applied to the Los Azufres spectral gamma fluctuation sequences by dividing the well-log sections into 27 intervals of 190 values over 30m for 01D and 140 values over 22m for 47D. As illustrated in Fig 12, interval Th/U fluctuation traces are associated interval fluctuation histograms. A ratio $\rho = \text{fluctuation-max/fluctuation-median}$ is determined for each interval, with the associated population distribution giving lognormality parameter α via best-fitting the empirical poroperm expression to the interval histogram (see Fig 12 red-line fits).

Figs 9-10 summarise the spatial association and lognormality-quantification of the Los Azufres Th/U abundance distributions for wells 01D and 47D: high intensity Th/U values registered in well-log abundance fluctuation sequences correspond to lognormally distributed fluctuation populations. It is thus plausible in a geocritical reservoir context to associate lognormally distributed solute abundances with high-permeability *in situ* flow structures capable of moving Th/U solutes over large-scale fracture-borne fluid pathways.

Figure 8. Progression of unit permeability distribution $\kappa = \exp(\alpha\phi)$ for increasing values of parameter α from small (upper left) to large (lower right); ϕ is normally distributed porosity.

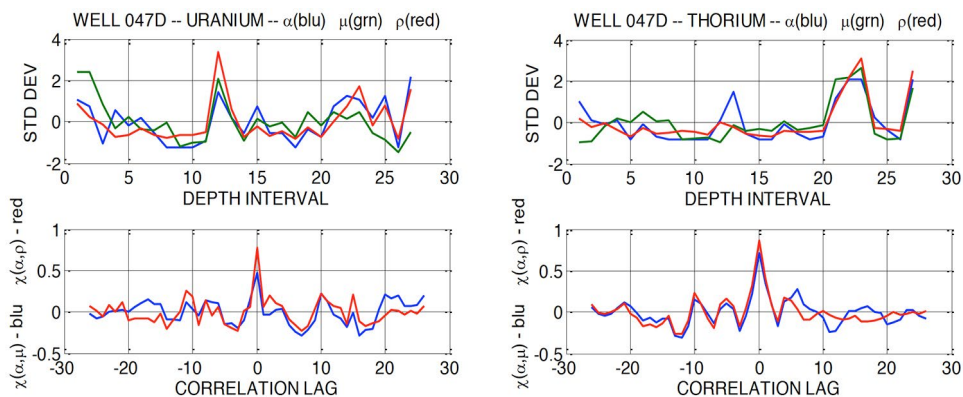


Figure 9. (Upper panels) Plot of lognormality parameter α , max-trace-amplitude μ , and max-amp/median-amp ratio ρ for intervals in well-log section along well-log section for respectively U/Th in well 47D; (lower panels) spatial correlation of lognormality parameter α , maximum abundance μ (blue) and maximum-abundance/median-abundance ratio ρ (red). 80% correlation of α and ρ in presence of large statistical noise affirms geocriticality expression $\kappa(x,y,z) = \kappa_0 \exp(\alpha(\phi(x,y,z) - \phi_0))$.

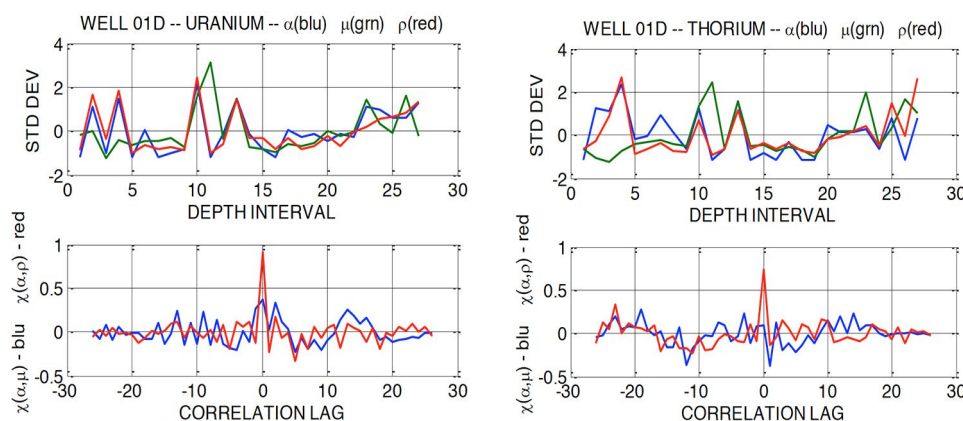


Figure 10. As Fig 9, for well 01D.

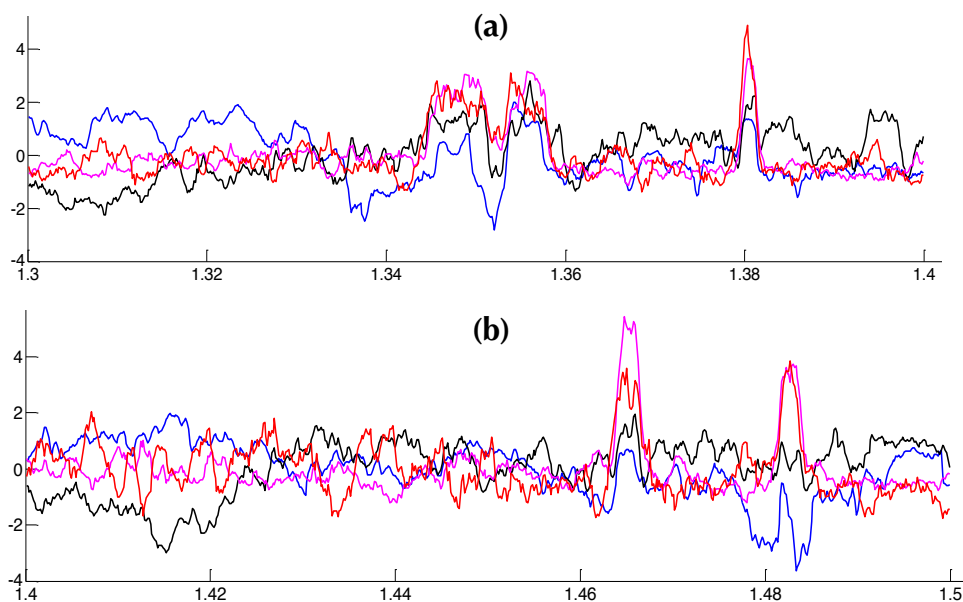


Figure 11. (a) Well 47D zero-mean/unit-variance traces for depth interval 1.3km to 1.4km; blue = porosity (solid) and density (dotted); black = P-wave and S-wave sonic velocities; red = K/Th/U gamma species abundances; (b) shows Th/U abundance traces with associated fitted histograms in six 22m intervals.

Fracture-Connectivity Origin of Th/U Well-Log Interval Over-Abundances

We have established a high (80%) degree of spatial correlation between occurrences of high-amplitude Th and U abundances (parameterized by $\rho = \text{fluctuation-max}/\text{fluctuation-median}$) for a well-log interval and a high degree of lognormality of well-log fluctuation amplitudes (parameterized by α in the empirical poroperm relation $\kappa = \kappa_0 \exp(\alpha\phi)$) for that interval. While a strong correlation between ρ and α is not statistically surprising, it usefully validates the relation $\kappa = \kappa_0 \exp(\alpha\phi)$ and helps establish a systematic means by which the observed species over-abundances can physically come about in geocritical poroperm media.

Focusing on the 200m well 47D interval at depths 1300m-1500m, Fig 11 juxtaposes four well-log traces rendered in zero-mean/unit-variance format: K = black; Th = magenta; U = red; reversed-polarity porosity = blue. In line with Figs 9-10, Fig 12 shows that lognormally distributed fluctuation amplitudes correspond with the Th/U over-abundance intervals shown in magenta (Th) and red (U).

The blue trace in Fig 11 shows that reversed-polarity porosity in well 47D correlates with Th/U over-abundances. However Fig A2 shows that porosity variation at Los Azufres is within 2% of a whole-well mean value $\sim 10\%$, hence it is plausible that low porosity correlation with solute over-abundance reflects silicification of a previously active flow structure. Fig 13 shows that porosity and sonic velocities are normally distributed in the 200m interval. Th/U abundances in Fig 11 are also essentially normally distributed except for the high abundance events in the 5m intervals at depth 1355m, and the 3m intervals at depths 1381m, 1465 and 1485m.

Whatever the material cause lying behind the Th/U over-abundance events, they do not register on density or sonic velocity channels, indicating that the over-abundances are not associated with significant local changes in mass density or elastic modulus; e.g., well-log evidence does not attribute Fig 11 Th/U over-abundances to high-fracture-density flow channels. Nor is it plausible from background fluctuations data that normalised Th/U over-abundances are of the same order if they appear in

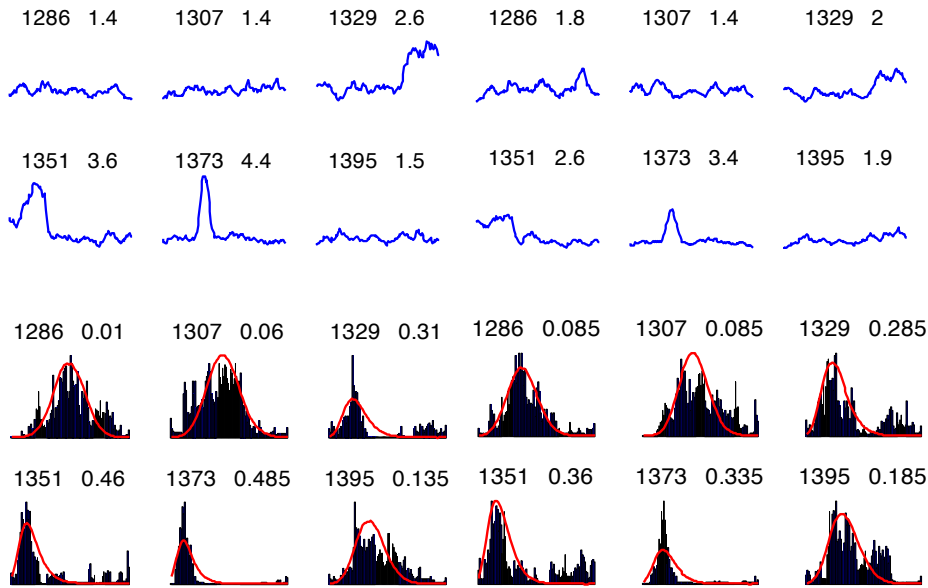


Figure 12. Well 47D Th/U abundance traces (upper panels) and associated histograms (lower panels) for six 22m intervals between ~1286m and ~1418m depths; abundance traces are normalised to overall well-log maximum; each trace and histogram plot titled with interval initial depth and with a plot datum; each trace datum is ratio $\rho = \text{max-abundance/med-abundance}$ for interval; each histogram datum is value of lognormality parameter α for interval; histograms are fit to distribution $\exp(\alpha\phi)$ for interval α and $\phi = \text{zero-mean/unit-variance normal distribution}$.

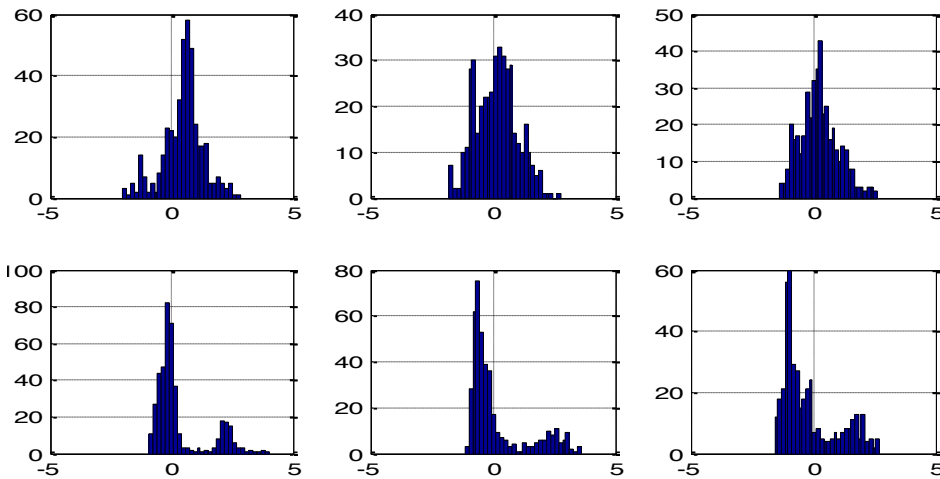


Figure 13. Well 47D well-log trace amplitude distributions in zero-mean/unit-variance normalised units for depth interval 1.3km to 1.4km as given in Fig 11; (left-right/upper) normally distributed P-wave sonic velocity, S-wave sonic velocity, porosity; (left-right/lower) lognormally distributed K, Th, U abundances.

an unusual geological rock type. Rather, as the amounts of Th/U are equally proportional to the mean abundance of each species, Fig 11 data argue in favor of a solute concentration mechanism in equilibrium with the mean background abundance of each species. In these circumstances, an acceptable physical mechanism for the observed over-abundance intervals is greater fracture-connectivity channelising fluid flow through an otherwise generic fractured rock volume. That is, well-log intervals of over-abundance of Th/U, and at times K, can be seen as part of a large-scale spatially erratic flow system within a geocritical crustal volume such as depicted in Fig 14.

A key observation is that localised wellbore K/Th/U over-abundances are (potentially) evidence for fracture-con-

nectivity pathways away from the wellbore. Through analysis of well-log K/Th/U distributions within a geocritical background of grain-scale fracture-density fluctuations recorded as ordinary degrees of fracture intensity fluctuation attested by the normally distributed sonic velocity and porosity data as in Fig 11, we can identify (possible) large-scale fracture-connectivity percolation flow networks in which a high degree of crust-wide fluid circulation has built up K/Th/U deposits.

Discussion

We have looked at well-log intervals of localized events of over-abundant solute species K/Th/U in the context of a ‘geocritical’ flow system characterized by a grain-scale fracture density distribution $n(x,y,z)$ governed by $N(k) \sim 1/k^\beta$, $\beta \sim 1$, a porosity distribution $\phi(x,y,z) \propto n(x,y,z)$ and a permeability distribution governed by $\kappa(x,y,z) = \kappa_0 \exp(\alpha(\phi(x,y,z) - \phi_0))$ for a fixed (or spatially variable) fracture connectivity parameter α . Governed by these constraints, a geocritical flow system posits flow as percolation via fracture connectivity flow paths on all scale lengths within a reservoir volume. In particular, *in situ* flow can be significantly enhanced along a fracture-connectivity pathway if the fracture-connectivity along the path is itself enhanced. In terms of the fracture-connectivity parameter α , such flow structures are marked by increased values of α rather than increased values of fracture density n or porosity ϕ . No other significant physical/material changes or structures need be in operation to signal increased flow due to increased fracture-connectivity marked by increased α . The sole marker of enhanced flow can be enhanced K/Th/U solute deposition within the fracture-connectivity pathway, with the accompanying statistical signature

of lognormal abundance distribution of well-log abundance data skewed to high populations of small abundances by the presence of a low-population of high-abundance outliers.

Fig 14 illustrates the spatial fluctuation nature of geocritical flow systems with their potential for enhanced flow to be signaled by enhanced K/Th/U deposition. Three important aspects of geocritical flow systems are:

- High degrees of spatially erratic flow paths, making drilling productive wells highly problematic (hence the well-attested lognormal distributions of well-productivity in oil/gas field (USEIA 2011) as well as geothermal fields (Grant 2009);

- The larger the flow-system scale, the larger are the associated permeability fluctuations (Leary et al 2012a), and hence the more costly the errors in reservoir management arising from uncertainty in reservoir flow structure.
- Los Azufres well-log Th/U abundance data show regions of the crust with evidence of higher fracture connectivity, i.e., high lognormality parameter α , than the norm, here shown yellow/red-tinted crustal section.

The Fig 14 aspects of the geocritical reservoir perspective emphasize the benefit of acquiring reliable large-scale knowledge of a reservoir flow system structure. We here speculate that, based on the Los Azufres sample K/Th/U abundance systematics, geothermal fields in which each well is logged for K/Th/U abundance can, particularly if the flow systems are active rather than in a relic/fossil state, help generate more effective reservoir flow models and thus benefit from previously unavailable flow structure spatial information.

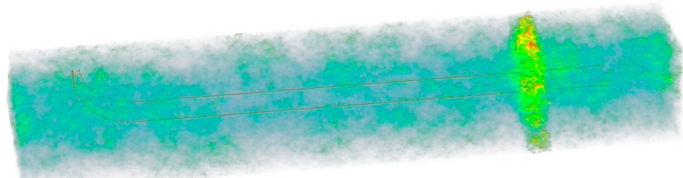


Figure 14. Generic synthetic geocritical crustal volume of nominal dimension 500m x 100m x 100m. Blue-green spatial fluctuations represent grain-scale fracture density spatial distribution conforming to Fourier spectral scaling $S(k) \sim 1/k^\beta$, $\beta \sim 1$, with associated permeability $\kappa(x,y,z) = \kappa_0 \exp(\alpha(\phi(x,y,z) - \phi_0))$ for nominal values of fracture-connectivity parameter α ; a region of enhanced α is high-lighted to yellow-green. Well logs traversing such a crustal volume record fluctuation distributions similar to those observed at Los Azufres.

Acquisition of large-scale flow structure data for currently active flow systems conforming to the K/Th/U signal present here can help build reliable reservoir simulation models by means of data assimilation with uncertainty quantification. The simulation models are constructed using all available flow-structure information, then updated sequentially in time interactively with incoming well pressure/flow information extracted from evolving reservoir observation. Data assimilation methods of choice are the ensemble Kalman filter (EnKF) and its variants (Aanonsen et al 2009; Bianco et al 2007) that progressively update a set of reservoir models from which flow-structure uncertainty parameters can be quantified. Uncertainty quantification is of utmost importance for reservoir production forecasts.

The means by which K/Th/U well-log flow-structure information is incorporated in reservoir management can be outlined as follows:

- Build a reservoir model from available geological, fault and well performance data;
- Embed the geological structure in a suite of generic geocritical reservoir fracture density distributions (e.g., Fig 14), using the geological, fault and well performance information to ‘seed’ or ‘bias’ the geocritical fracture-density distributions towards lower or higher flow-permeability depending of the data;

- K/Th/U flow structure data (e.g., highlighted portions of Fig 14) supplement previously available well-log fracture-density/porosity/resistivity data by indicating flow structural zones of significantly increased fracture-connectivity parameter α .
- Using data assimilation methods such as EnKF, simulate flow in the reservoir for the suite of geocritical reservoir models, giving specific attention to matching flow realisations to K/Th/U abundance data if these structures are active;
- Analyse the results and the associated uncertainty quantification;
- Generate production forecasts based upon the latest updated reservoir simulation models.

Acknowledgement

We gratefully acknowledge Gerencia de Proyectos Geotermoelectricos de Comisión Federal de Electricidad for free access to Los Azufres well-log and related data and generous permission to publish findings based on those data. We thank Dr John Rugis for his construction of Figure 14.

References

- Aanonsen SI, Nævdal G, Oliver DS, Reynolds AC & Vallès B (2009) The Ensemble Kalman Filter in Reservoir Engineering, *SPE Journal* 14, No 3, 393-412; SPE-117274-PA.
- Bianco A, Cominelli A, Dovera L, Nævdal G & Valles B (2007) History Matching and Production Forecast Uncertainty by Means of the Ensemble Kalman Filter: A Real Field Application, EUROPEC/EAGE Conference and Exhibition, 11-14 June, London.
- Clark SP (1966) *Handbook of Physical Constants (revised)*. Geol. Soc. America Mem. 97, pp587.
- Grant MA (2009) Optimization of drilling acceptance criteria, *Geothermics* 38, 247-253.
- Gutierrez A & Aumento F (1982) The Los Azufres, Michoacan, Mexico, geothermal field, *Journal of Hydrology* 56, 1-2, 137-145, 147, 149-162
- Leary PC (2002) Fractures and physical heterogeneity in crustal rock, in *Heterogeneity of the Crust and Upper Mantle – Nature, Scaling and Seismic Properties*, J. A. Goff, & K. Holliger (eds.), Kluwer Academic/Plenum Publishers, NewYork, 155-186.
- Leary PC (1997) Rock as a critical-point system and the inherent implausibility of reliable earthquake prediction, *Geophysical Journal International* 131, 451-466.
- Leary PC (1991) Deep borehole log evidence for fractal distribution of fractures in crystalline rock. *Geophysical Journal International* 107, 615-628.
- Leary P., P. Malin & J. Pogacnik (2012a) Computational EGS -- Heat transport in 1/f-noise fractured media, *37th Stanford Geothermal Workshop*, Stanford CA, 30Jan – 1Feb.
- Leary P, Pogacnik J & Malin P (2012b) Fractures ~ Porosity → Connectivity ~ Permeability → EGS Flow Stimulation, *Proceedings Geothermal Resources Council 36th Annual Conference*, Reno, 30Sep – 3Oct.
- Leary P.C. & L.A. Walter (2008) Crosswell seismic applications to highly heterogeneous tight gas reservoirs, *First Break* v.26, 33-39.

Leary PC & Al-Kindy F (2002). Power-law scaling of spatially correlated porosity and log(permeability) sequences from north-central North Sea Brae oilfield well core, *Geophysical Journal International*, 148, 426-442.

Pogacnik J., P. Leary & P. Malin P, 2012. Computational Framework for EGS Fracture Stimulation, 36th *Geothermal Resources Council Annual Meeting*, Reno, 30Sep – 3Oct.

Leary PC, Malin PE, Pogacnik JA, Rugis J, Valles B, Geiser P, Lacazette A & Vermilye J (2013) The GeoCritical Reservoir – Observing/Modeling Long-Range & Lognormally Distributed Permeability Structures in Crustal Fracture/Flow Systems, submitted to *Bulletin of American Association of Petroleum Geologists*.

Molina Martínez A (2009) Assessment of the northern part of the Los Azufres geothermal field, Mexico, by lumped parameter modeling and Monte Carlo simulation, *Geothermal Training Programme Reports*, No18, IS-108 Reykjavik, Iceland.

Stimac JA (2007) Properties of the Bulalo Geothermal Reservoir Top based on Core Analysis, *Proceedings 29th NZ Geothermal Workshop*.

US Energy Information Administration (2011) Distribution and Production of Oil and Gas Wells by State, www.eia.gov/pub/oil_gas/petroleum/all-years-states.xls.

APPENDIX 1

Los Azufres well-log data spectral trends attest to the power-law scaling character of the geological formations sampled by wells 01D and 47D, $S(k) \sim 1/k^\beta$, $\beta \sim 1.4$.

Los Azufres porosity well-log for well 01D shows porosity confined to the vicinity of 10% with only the upper part of the well section exceeding 13% porosity; it is thus unlikely that

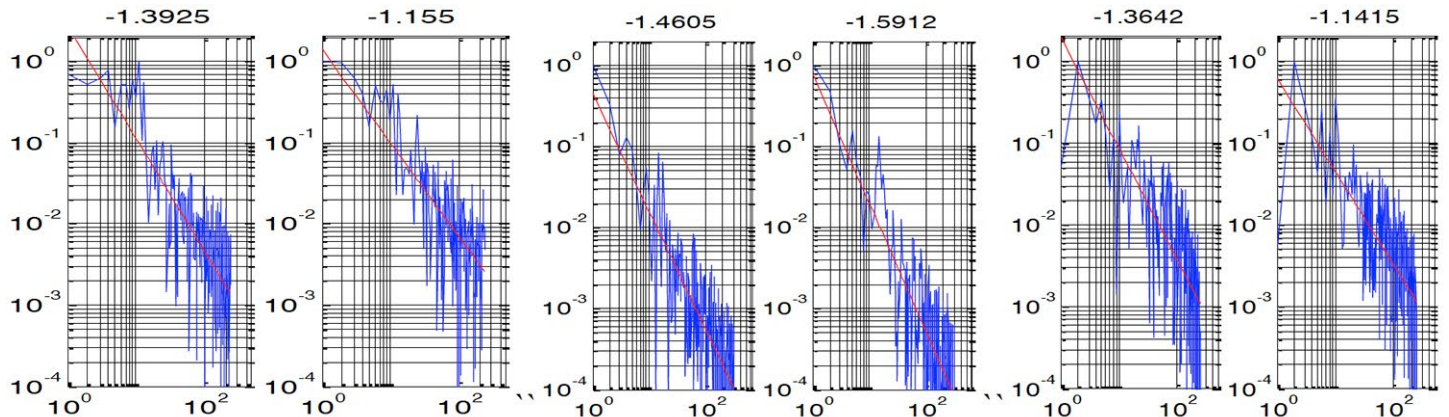


Figure A1. Well 47D well-log power-law spectra for (left to right) P, S sonic velocity, porosity, mass density, Th and U. Mean $\beta = 1.34$ Std $\beta = 0.17$.

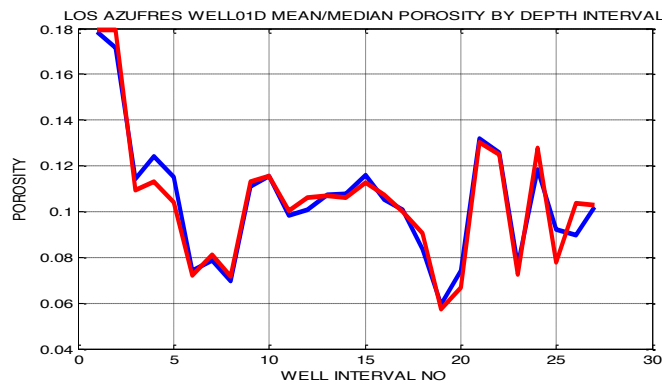


Figure A2. Interval mean porosity values for well 01D.

porosity difference between formations per se provides significant differences in flow with the reservoir.

Plots/histograms from well-core data from geothermal fields in New Zealand (IESE unpublished data) and the Philippines (Stimac 2007) are consistent with the well-core poroperm fluctuation relation $\delta\phi \sim \delta\log(\kappa)$ and lognormality widely observed for clastic reservoir well-core data.

Figure A3 (below). (Left, center) Normalised porosity (blue) and log(permeability) (red) for Ohaaki geothermal field, New Zealand, and Bulao geothermal field, Philippines; (right) porosity (left) and permeability (right) histograms, ~normal for porosity, ~lognormal for permeability.

